POTENTIAL OF THE J-PET DETECTOR FOR STUDIES OF DISCRETE SYMMETRIES IN DECAYS OF POSITRONIUM ATOM — A PURELY LEPTONIC SYSTEM

P. Moskal[a], D. Alfs[a], T. Bednarski[a], P. Białas[a], E. Czerwiński[a]

C. Curceanu[b], A. Gajos[a], B. Głowacz[a], M. Gorgol[c]

B.C. Hiesmayr[d], B. Jasińska[c], D. Kamińska[a], G. Korcyl[a]

P. Kowalski[e], T. Kozik[a], W. Krzemień[f], N. Krawczyk[a]

E. Kubicz[a], M. Mohammed[a], Sz. Niedźwiecki[a]

M. Pawlik-Niedźwiecka[a], L. Raczyński[e], Z. Rudy[a], M. Silarski[a]

A. Wieczorek[a,g], W. Wiślicki[e], M. Zieliński[a]

[a]Faculty of Physics, Astronomy and Applied Computer Science
Jagiellonian University, 30-348 Kraków, Poland
[b]INFN, Laboratori Nazionali di Frascati
CP 13, Via E. Fermi 40, 00044, Frascati, Italy
[c]Department of Nuclear Methods, Institute of Physics
Maria Curie-Skłodowska University, 20-031 Lublin, Poland
[d]Faculty of Physics, University of Vienna
Boltzmanngasse 5, 1090 Vienna, Austria
[e]Świerk Computing Center, National Center for Nuclear Research
05-400 Otwock-Świerk, Poland
[f]High Energy Physics Division, National Center for Nuclear Research
05-400 Otwock-Świerk, Poland
[g]Institute of Metallurgy and Materials Science, Polish Academy of Sciences
30-059 Kraków, Poland

The Jagiellonian Positron Emission Tomograph (J-PET) was constructed as a prototype of the cost-effective scanner for the simultaneous metabolic imaging of the whole human body. Being optimized for the detection of photons from the electron–positron annihilation with high time- and high angular-resolution, it constitutes a multi-purpose detector providing new opportunities for studying the decays of positronium atoms. Positronium is the lightest purely leptonic object decaying into photons. As an atom bound by a central potential, it is a parity eigenstate, and as an atom built out of an electron and an anti-electron, it is an eigenstate of the charge conjugation operator. Therefore, the positronium is a unique laboratory to study discrete symmetries whose precision is limited, in principle, by the effects due to the weak interactions expected

at the level of ($\sim 10^{-14}$) and photon–photon interactions expected at the level of ($\sim 10^{-9}$). The J-PET detector enables to perform tests of discrete symmetries in the leptonic sector via the determination of the expectation values of the discrete-symmetries-odd operators, which may be constructed from the spin of ortho-positronium atom and the momenta and polarization vectors of photons originating from its annihilation. In this article, we present the potential of the J-PET detector to test the C, CP, T and CPT symmetries in the decays of positronium atoms.

1. Introduction

If Nature was utterly symmetric, the matter would not exist. Thus, we owe our existence to the asymmetry between matter and anti-matter which must have appeared at the early stage of the evolution of the Universe. Surprisingly though, processes driven by the gravitational, electromagnetic and strong interactions up to now appear to be symmetric with respect to reflection in space (P), reversal in time (T) and charge conjugation (C). So far, violations of these symmetries were observed only in processes governed by the weak interaction. Breaking of C and CP symmetries is a necessary condition for baryogenesis to occur (for generation of asymmetry between baryons and anti-baryons), independently of the particular mechanism [1]. Yet, the excess of matter over anti-matter which we observe in the current Universe is by about nine orders of magnitude too large with respect to the theoretical estimations based on the presently known sources of the discrete symmetries violations [2]. This huge discrepancy remains one of the greatest puzzles in physics and cosmology.

The origin of the excess of matter over anti-matter in the Universe may also be explained by the leptogenesis [3] which is referred to as the hypothesis explaining the existence of the matter in the Universe by the appearance of lepton–anti-lepton asymmetry in the early stage of its evolution. The present theory of leptogenesis postulates that lepton–anti-lepton asymmetry was generated in decays of the hypothetically heavy right-handed neutrinos and it was converted to the baryon–anti-baryon asymmetry via interaction of hypothetical sphalerons [4]. However, the existence of both mentioned particles was not confirmed up to now. Interestingly, though the matter which we know is made of quarks and leptons, violation of CP and T symmetries have been observed only for systems including quarks, and it has not yet been discovered in any processes involving purely leptonic matter. Such studies are challenging and the best so far performed experiments with positronium atoms excluded violation of discrete symmetries as CP, T or CPT only at the level of about 0.3% [5, 6], which is many orders of magnitude less precise than the accuracies achieved in the quark sector.

By using the J-PET detector, we plan to investigate symmetries in the decays of positronium (e^+e^-) which is composed of lepton and anti-lepton constituting the simplest atom made of matter and anti-matter.

This article is organized as follows: first, we describe the basic properties of the positronium atom, next, we present the state of the art and detailed justification for C, CP, T and CPT symmetries breaking. Further on, we explain the principle of operation of the J-PET tomograph including introduction of methods developed for the creation of spin- and tensor-polarized positronium atoms. Next, we describe the techniques for monitoring of the linear and tensor polarization of positronium atoms, as well as the method for the determination of photons polarization. This description is followed by an estimate of the limitations for the discussed studies due to the instrumental and physical backgrounds. Finally, we introduce odd-symmetric operators (constructed from ortho-positronium spin, as well as momentum and polarization vectors of photons) which will be used for the tests of the discrete symmetries.

It is important to stress that the tests of symmetries with positronium described hereafter in this article are independent of and thus not limited by the results of the tests for T and CP invariance in muon decays (*e.g.* $\mu \to e\nu\bar{\nu}$) and by the searches of the electric dipole moments [7].

2. Positronium

Positronium [8] is simultaneously an atom and an anti-atom. It is built out of an electron and an anti-electron, and thus it is a purely leptonic object. Similarly as atoms bound by a central potential, it is an eigenstate of the parity operator P. In addition, unlike the ordinary atoms, but similarly to the flavor neutral mesons, the positronium is symmetric under the exchange of particles into anti-particles and so it is also an eigenstate of the charge conjugation operator C and thus an eigenstate of the CP operator. It is the simplest atomic system with charge conjugation eigenstates [9]. This makes it ideal for studies of the discrete symmetries in Nature.

Positronium, similarly to the hydrogen atom, in the ground sub-states with orbital angular momentum $L = 0$, is formed in a singlet state of the anti-parallel spins orientation, the so-called para-positronium (p-Ps), or in a triplet state of parallel spin orientation, the so-called ortho-positronium (o-Ps). Due to the symmetry of charge conjugation, p-Ps undergoes annihilation with emission of an even number of photons (most often, two photons), while o-Ps undergoes annihilation with emission of an odd number of photons (most often, three photons). Therefore, due to the smallness of the fine-structure coupling constant and to the differences in phase space volume available for decays into different number of photons, the average

lifetimes of o-Ps and p-Ps differ by more than three orders of magnitude. The lifetime of p-Ps in a vacuum is equal to $\tau_{p-Ps} \approx 0.125$ ns [10], whereas the average lifetime of o-Ps amounts to $\tau_{o-Ps} \approx 142$ ns [9, 11, 12]. Such large difference in lifetimes enables a very efficient experimental disentangling of these states.

3. Motivation to test discrete symmetries in decays of positronium atoms

3.1. Tests of charge conjugation symmetry

Violation of C symmetry in gravitational, strong and electromagnetic interaction was not observed so far. The best limit in systems of quarks was set for $\pi^0 \rightarrow 3\gamma$ decay and amounts to 3.1×10^{-8} at 90% C.L. [13, 14]. In the framework of the J-PET experiment, we intend to study the C symmetry in the leptonic system searching for the C-forbidden decays of the positronium atoms. Positronium, as a system of fermions, must be anti-symmetric under exchange of its components. Thus, as mentioned in the previous section, ground state of ortho-positronium as symmetric in space ($L = 0$) and in spin ($S = 1$) must be C-symmetry odd, and para-positronium as symmetric in space and anti-symmetric in spin ($S = 0$) must be C-symmetry even. Photons are C-odd and thus the C eigenvalue of n photons is equal to $(-1)^n$. Therefore, C symmetry forbids decays of ortho-positronium into even number of photons and para-positronium into an odd number of photons. It is important to stress that such decays cannot occur due to the possible mixing between various positronium states because there are no different positronium states with the same J^P and opposite C parity [9]. The branching ratio for these decays (calculated based on the Standard Model) is of the order of 10^{-10}–10^{-9} [7, 15]. Hence, observation of the branching ratio for *e.g.* o-Ps $\rightarrow 4\gamma$ or p-Ps $\rightarrow 3\gamma$ significantly greater than expected on the basis of the Standard Model would suggest violation of the C symmetry by the electromagnetic interactions. So far, we know only upper limits of these branching ratios amounting to:

$$\mathrm{BR(o\text{-}Ps \rightarrow 4\gamma / o\text{-}Ps \rightarrow 3\gamma)} < 2.6 \times 10^{-6} \quad \text{at} \quad 90\% \text{ C.L. [16]},$$
$$\mathrm{BR(p\text{-}Ps \rightarrow 3\gamma / p\text{-}Ps \rightarrow 2\gamma)} < 2.8 \times 10^{-6} \quad \text{at} \quad 68\% \text{ C.L. [17]},$$
$$\mathrm{BR(p\text{-}Ps \rightarrow 5\gamma / p\text{-}Ps \rightarrow 2\gamma)} < 2.7 \times 10^{-7} \quad \text{at} \quad 90\% \text{ C.L. [18]},$$

where the best limit [18] was achieved in the Lawrence Berkeley National Laboratory in USA by means of the Gammasphere detector, a spectrometer for nuclear structure research [18]. These values are still more than two orders of magnitude larger than expected for the C-conserving process which would imitate C-violation due to the vacuum polarization effects.

3.2. Tests of CP symmetry

The violation of the CP symmetry has been observed for the first time in 1964 in the decays of K_L mesons [19]. Interestingly, the CP violation in K_S mesons has not been observed so far. The best limit was set by the KLOE-2 Collaboration in 2013 [20, 21]. K mesons remained the only systems for which such violation had been observed for almost forty years. First indications of the CP violation in the B mesons decays were reported only in the year 2001 by the Belle Collaboration at KEK in Japan [22] and by the BaBar Collaboration at Stanford Linear Accelerator Center SLAC in USA [23]. In 1973, Kobayashi and Maskawa [24] explained the CP violation in quark systems via the presence of the complex phase in the quark transition matrix, extending the model of Cabibbo [25], and suggesting the existence of three quark generations (at those days only u, d and s quarks were known but indeed c, b, and t quarks were discovered later). For this achievement, Kobayashi and Maskawa were awarded the Nobel Prize in 2008. Sakharov has argued that the violations of C and CP symmetries are necessary requirements for the explanation of the observed excess of matter over anti-matter [1]. However, the presently known sources of the CP symmetry violations are still by far too small and can account for only about 10^{-9} fraction of the observed excess of matter over anti-matter [2]. Therefore, many particle physics experiments as *e.g.* LHCb experiment [26] at CERN or Belle-II experiment [27] at KEK plan to search for CP symmetry violation effects in hadrons with upgraded detectors and beam intensities.

Though the violation of the CP symmetry is small, it has been shown in several contributions that it has a crucial impact on various domains in physics. For instance, the role of time is still puzzling and controversial; whereas in Quantum Mechanics, the position is well-described in theory by an operator, time usually is treated as a parameter. Time operator models exist, in particular a certain one denoted the temporal wave function model that extends the Born rule to the time domain [28]. It had been in no conflict with any known experiment; indeed, the falsification of the model turned out to be due to the violation of the CP symmetry [28], though tiny. Another example is given by showing that correlations stronger than those allowed by classical physics are related to the violation of the CP symmetry [29, 30] and thus, in principle, providing the security for quantum cryptographic protocols [31].

The search for CP violation was conducted also in other systems, as *e.g.* in the $\eta \to \pi^+\pi^- e^+ e^-$ decay [32] which does not change the flavor quantum number. Such CP symmetry breaking is not included in the Standard Model. This CP non-conservation would manifest itself in the asymmetry in the angular distribution between the emission planes of $e^+ e^-$ and $\pi^+\pi^-$ pairs. So far, such a violation was not observed and the most accurate results were

obtained with the KLOE experiment [33]. Concurrently, other experiments may test the CP-symmetry violation in processes involving purely leptonic systems. To this end, in the USA, neutrinos from Fermilab are sent to NOvA detector [34] 810 km away, and in Japan the T2K Collaboration [35] sends neutrinos from J-PARC in Tokai to 295 km away Super-Kamiokande detector in Kamioka. The most sensitive signature of the CP-symmetry violation which is expected from these experiments is a difference between the probability of muon neutrino oscillations into electron neutrino $P(\nu_\mu \to \nu_e)$ and the probability of its CP symmetric process which is oscillations of muon anti-neutrino into electron anti-neutrino $P(\bar{\nu}_\mu \to \bar{\nu}_e)$. However, it is estimated [36, 37] that NOvA and T2K experiments can provide a CP-violation discovery potential up to 2σ only in the year 2020 and up to 3σ in 2024. Thus, the study of the CP-symmetry violation in lepton systems is one of the most exciting challenges of todays particle physics.

We intend to use the J-PET detector to search for CP-symmetry violation in decays of positronium atoms. We plan to measure the expectation value of the CP-odd operators constructed from the momentum and polarization vectors of photons and polarization of positronium atoms. Examples of such operators are given hereafter in Table I. Observation of the non-zero expectation value of the CP-odd operator would imply the CP non-invariance. There is a very strong limitation on the electric dipole moment of electron $|d_e| < 10.5 \times 10^{-28}\, e$ cm at 90% C.L. [13, 38]. It puts limitations of the order of 10^{-18} [39] on CP violation driven by the Standard Model mechanisms such as *e.g.* one-photon exchange $ee\gamma$ or $ee2\gamma$ and $ee3\gamma$ processes. However, it does not preclude a possible much larger violation of CP symmetry in the positronium annihilation due to exotic non-Standard Model mechanisms [40]. On the other hand, the photon–photon interaction in the final state due to the vacuum polarization may mimic CP non-invariance on the level of 10^{-9} [7, 15], and effects due to the weak interaction can lead to a violation at the order of 10^{-14} [9]. The present best upper limit on the CP violation in the decays of ortho-positronium atoms was determined at the University of Tokyo and amounts to 4.9×10^{-3} at 90% C.L. [5]. Thus, there is still more than six orders of magnitude difference between the present experimental upper limit and the CP violation expected due to the photon–photon interaction.

3.3. Tests of T symmetry (time reversal invariance)

Time reversal symmetry (T) is epistemologically extremely attractive. However, although one can reverse the direction of the motion in space, one cannot reverse the direction of the elapsing time. Therefore, in order to study the time reversal violation, one investigates expectation values for the T-odd

operators of the non-degenerate stationary states [41] as *e.g.* electric dipole moment (EDM) of the particles with spin, or one compares processes which are related by exchange of initial and final states equivalent to reversing the time. In the latter case, one reverses only a motion and, therefore, the time reversal invariance is often referred to as motion reversal symmetry [41]. For such studies, the anti-unitary character of the T operator makes the experimental studies of the time reversal invariance more challenging than other symmetries [41], since it requires abilities of preparing the initial and final states of the process in a fully controlled way.

Only recently in 2012, in the experiment conducted by the BaBar Collaboration with the use of the SLAC linear accelerator at Stanford University, the time reversal violation was observed independently of the CP or CPT symmetries [42]. Based on the quantum entangled B mesons produced in the decays of the $Y(4S)$ meson and using the ideas described in Ref. [43], the BaBar group has shown that the probabilities of the time reversal symmetric transitions between the flavor eigenstates $(B_0, \bar{B}_0)$ and CP eigenstates (B_+, B_-) are different. For example, it was shown that the probability of the transition between flavor $\bar{B}^0$ and CP $= -1$ states $(\bar{B}^0 \to B_-)$ is different from the probability for its T symmetric process: $B_- \to \bar{B}^0$. Importantly, T, CP and CPT symmetries applied to the $\bar{B}^0 \to B_-$ transition lead to the different processes: $\text{T}(\bar{B}^0 \to B_-) = B_- \to \bar{B}^0$; $\text{CP}(\bar{B}^0 \to B_-) = B^0 \to B_-$; $\text{CPT}(\bar{B}^0 \to B_-) = B_- \to B^0$. The obtained result is consistent with the level of CP-symmetry violation and the assumption of the CPT conservation.

So far, none of the experiments reported limits on the T-symmetry violations in the decays of positronium. The known final state interactions of photons are expected to mimic the T violation at the level of 10^{-9} [7, 15]. All of the previous investigations with positronium, which tested the discrete symmetries odd operators, were based on the products of photons momenta and positronium spin vectors. We plan to extend the study to other operators, taking advantages of properties of the J-PET tomography scanner, which enables to determine the polarization of photons (see Section 4.5). Therefore, using the J-PET detector, the T symmetry can be investigated by searching for the possible non-zero expectation values of the T-odd operators which can be constructed from momentum and polarization directions of photons originating from the decays of the o-Ps atoms as well as from the spin of these atoms (see Section 5).

It is important to stress that so far all experiments searching for the non-zero expectation value of the T-odd operators provided no signals of T-symmetry violation and hence the K and B mesons remain the only systems for which the time reversal symmetry violation was observed.

3.4. Tests of CPT symmetry

CPT symmetry being combination of the above described discrete symmetries of charge conjugation C, spatial parity P and reversal in time T, constitutes a fundamental law of quantum field theory resulting from the locality and unitarity of interactions and from the Lorentz invariance [44, 45]. There are known processes breaking invariance of C, P and T separately, and even few processes breaking combined CP symmetry, but so far violation of CPT invariance has not been observed. The breaking of this symmetry would imply violation of one or more of the above mentioned fundamental assumptions, and at the same time, as proven by Greenberg, it would imply the breaking of the Lorentz symmetry [46]. We cannot *a priori* exclude that unitarity, locality or Lorentz invariance are not broken in the regime of very high energies, where the quantum gravity effects may play a significant role [47]. There exist many unverified models and theories among which, as an example, it is worth to mention the extensions of the Standard Model non-invariant with respect to CPT and Lorentz symmetry as proposed by Kostelecky [48]. However, it is not possible for the moment to predict precisely how such effects could manifest themselves in phenomena involving particles and anti-particles at energies available in laboratories. Searching for CPT symmetry breaking in processes involving various kinds of particles should be treated as complementary. Therefore, in many physics laboratories, CPT invariance is tested in various physical systems, for example, via comparison of meson and its anti-meson properties [49], or via comparison of properties of hydrogen and anti-hydrogen [50–53]. Some of the most sensitive tests were made [54] and are planned [33] based on the quantum interferometry of entangled neutral kaons [55].

It is worth noting that with respect to the quark sector, relatively poor experimental limits of CPT-symmetry violation were achieved in processes involving decays of positronium atoms. The best limit so far on the CPT violation in positronium decays was set on the level of 0.3% and it was obtained using the Gammasphere array of Compton suppressed high-purity germanium detectors [6]. Thus, this is still six order of magnitude larger than the possible contribution from radiative corrections which may mimic CPT violation at the level of 10^{-9} [15]. Analogously, as in the case of the above discussed CP and T symmetries, the tests of CPT invariance will be conducted using the J-PET detector via the measurement of the expectation values of the CPT-odd operators listed in Table I.

4. J-PET: Jagiellonian Positron Emission Tomograph

The J-PET scanner is built out of strips of organic scintillator, forming a cylinder (left panel of Fig. 1) [56, 57]. Light signals from each strip are
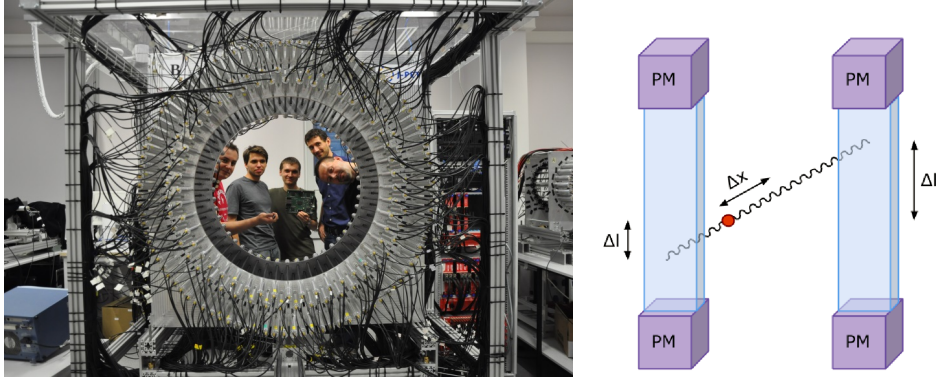
Fig. 1. (Left) Photo of the J-PET detector with a few members of the J-PET group. The active inner part of the detector has a cylindrical shape with the length of 50 cm and diameter of 85 cm. The J-PET tomography scanner is made of three layers of plastic scintillator strips wrapped with the Vikuiti specular foil covered with an additional light-tight foil (black). The scintillators are optically connected at two ends to Hamamatsu R9800 vacuum tube photomultipliers (gray). (Right) Schematic view of the two detection modules [58]. A single detection module consists of a EJ-230 scintillator strip read out by two photomultipliers labeled PM. In the first approximation, the hit distance from the center of the scintillator (ΔL) is determined based on time difference measured at both ends of the scintillator strip. In the case of the two-photon annihilation, the position (Δx) along the line of annihilation is determined from time difference measured between two modules. In practice, more advanced methods of hit-time and hit-position were developed which take advantage of the variation of the signal shape as a function of the hit-position [58–60]. In the case of three photon annihilation, the positronium decay point is reconstructed based on the trilateration method [61].

converted to electrical signals by photomultipliers placed at opposite ends of the strip [62]. The position and time of reaction of photons in the detector material is determined based on the arrival time of light signals to the ends of the scintillator strips (right panel of Fig. 1). The signals are probed in the voltage domain with the accuracy of about 30 ps by a newly developed multi-threshold digital electronics [63, 64] and the data are collected by the novel trigger-less and reconfigurable data acquisition system [65–67]. The readout data is streamed to the Central Controller Module and then, further, to permanent storage [66]. For the data processing and simulations, a dedicated software framework was developed [68–70]. The hit-position and hit-time of photons in the scintillator strips are reconstructed by the dedicated reconstruction methods based on the compressive sensing theory [59, 60] and the library of synchronized model signals [58, 71, 72]. The hit-time and hit-

position reconstruction procedures are further developed, but it is important to note that at present, the achieved resolution for the determination of the hit-time of the annihilation photons is about 0.1 ns for energy deposition about 0.27 MeV [58, 62].

4.1. Positronium production

Positronia will be produced by positrons interacting with electrons in the porous materials. Three different kinds of positronium targets are planned to be prepared, which will be optimized for the production of *(i)* unpolarized positronium atoms, *(ii)* linearly spin-polarized positronium atoms, and *(iii)* tensor spin-polarized positronium atoms. In each case, a beta-plus radioactive isotope of ^{22}Na is planned to be used as positrons source. However, for some tests of systematic effects, we consider also the use of ^{68}Ge and ^{44}Sc [73] isotopes. For the production of unpolarized and spin-tensor polarized positronium, a radioisotope ^{22}Na affixed in 7.5 μm Kapton foil will be used. The source will be inserted between two layers of target material (sandwich configuration), as it is depicted schematically in the left panel of Fig. 2. The positronium produced in the material may disintegrate not only via internal annihilation, but also due to the interaction with electrons
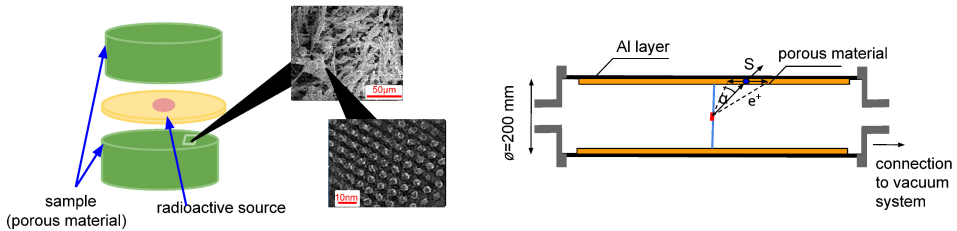

Fig. 2. (Left) Pictorial presentation of the positronium source with the radioactive isotope surrounded by the porous material. Inserted figures were taken for the SBA-15 porous material using SEM (upper figure) and TEM (lower one) techniques. Bars indicate 50 μm (upper figure) and 10 nm (lower figure). The positronium source will be kept in the annihilation chamber with the vacuum sufficient to suppress effectively ortho–para conversion with paramagnetic molecules of air. (Right) Schematic view of a spin-linear polarized positronium target in the form of cylinder surrounding the positron source. Longitudinally polarized positrons are emitted from the beta-plus radioactive source placed in the center of the cylinder. Ortho-positronium atoms with spin $\vec{S}$ are formed in the cylindrical layer of the porous material. The direction of the polarization will be determined with the uncertainty of $\pm \alpha$ determined by the precision of the o-Ps annihilation point reconstruction using a trilateration-based method introduced recently in reference [61].

from surrounding molecules. Therefore, in order to minimize systematic uncertainties in studies of the symmetries violation in the ortho-positronium decays, the lifetime of ortho-positronium and its production probability in the material should be maximized [74]. More specifically, the fraction ($f_{3\gamma}$) of o-Ps $\rightarrow 3\gamma$ decay rate to the overall annihilation rate, as well as the fraction of events from ortho-positronium decays to all the 3γ annihilations ($f_{3\gamma}$(o-Ps) = N(o-Ps $\rightarrow 3\gamma$)/$N(3\gamma)$) should be as large as possible. The best known materials for such experiments are silica aerogels [75, 76] in which empty space constitutes more than 90% of the total volume [77]. Recently, we have performed studies [74] by measuring the lifetime and production probability of ortho-positronium atoms, as well as the 3γ fraction of their annihilation in samples of commercial aerogels (IC3100, IC3110, IC3120 and LA1000), Amberlite porous polymer XAD4 (CAS 37380-42-0) and silica porous material SBA-15 synthesized in the Faculty of Chemistry of Maria Curie-Skłodowska University [78]. We found that the lifetime is the largest for the aerogel IC3100 and amounts to about 132 ns, and that the fractions $f_{3\gamma}$ and $f_{3\gamma}$(o-Ps) are the largest for the XAD-4 porous polymer. In particular, we observed that for this polymer, the fraction $f_{3\gamma}$ varies between 24.4% to 28.9% depending on the measurement method, and that $f_{3\gamma}$(o-Ps) is as large as 99.7% [74].

4.2. Linear polarization of ortho-positronium atoms

The geometry and properties of the J-PET detector enable to design the positronium source such that the vector polarization of produced ortho-positronium can be determined. Due to the parity violation in the beta-decay, the emitted positrons are longitudinally polarized with the polarization vector equal to $\vec{P} = \vec{v}/c$, where $\vec{v}$ denotes the positron velocity. This effect was used *e.g.* in the Gammasphere experiments where the target was built from a hemisphere of silicon dioxide aerogel with the radioactive source in the center of the sphere [6]. For the J-PET experiment, we plan to construct a spin-polarized positronium source as shown in the right panels of Fig. 2 and Fig. 3.

The positron emitted from the source placed in the center of the detector interacts in the cylindrical layer of the porous material. The created positronium annihilates into three photons (see Fig. 3) and the time and position of their interactions in the scintillator strips enables to reconstruct the position of annihilation by means of the trilateration method. The trilateration-based reconstruction of ortho-positronium annihilation position and time was recently introduced in references [61, 79]. Detailed simulations taking into account the properties of the J-PET detector indicate that this method enables to reconstruct the annihilation position with the spatial resolution of
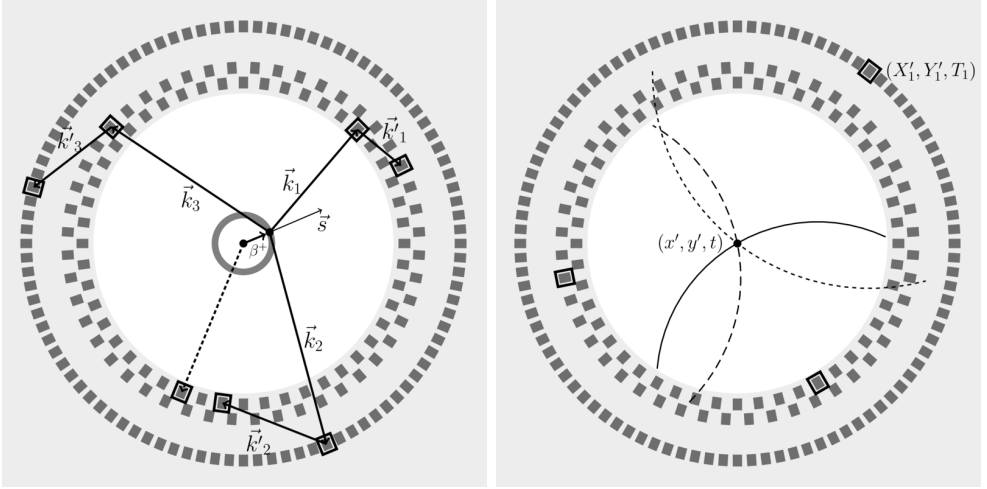
Fig. 3. (Left) Schematic view of the cross section of the J-PET detector (rectangles) with the linearly polarized positronium source indicated as a circle surrounding the center. A projection onto the plane perpendicular to the detector axis is shown. Source may be realized as an aerogel cylinder (see Fig. 2) whose diameter, housing material and thickness still need to be optimized. Superimposed arrows indicate momentum and spin vectors involved in the typical event of ortho-positronium production with spin ($\vec{S}$). A black dot in the center indicates a sodium ^{22}Na radioactive source emitting longitudinally polarized positron ($\vec{\beta^+}$) from parity violating beta-decay and prompt gamma quantum (dotted arrow) from the de-excitation of daughter nucleus ^{22}Ne. Positronium (dot marked in the cylinder) decays into three photons ($\vec{k_1}, \vec{k_2}, \vec{k_3}$). Each photon may interact via Compton effect in the scintillator strips (marked by rectangular rims), and the secondary photons ($\vec{k_1'}, \vec{k_2'}, \vec{k_3'}$) may also react in the scintillator strips. (Right) Scheme of the reconstruction of ortho-positronium annihilation time and point (x', y', t) inside the decay plane. Hit-positions (rectangular rim surrounding the hit scintillator strip) for each recorded photon constitute the center of a circle (e.g. X_1', Y_1', T_1) describing possible photon origin points where radius of the circle depends on the difference between the hit-time and the annihilation time t. The decay point is found as an intersection of the three circles. The right figure is adapted from reference [61].

about 1 cm to 2 cm [61], and the annihilation time with the resolution of about 0.1 ns [61]. In the Global Positioning System (GPS), a trilateration is based on measurements of time and position of signals by four satellites. In the case of the reconstruction of ortho-positronium location, the lack of a fourth reference system is compensated by the momentum conservation which implies that the decay point of ortho-positronium (o-Ps $\rightarrow 3\gamma$) and the momentum vectors of photons are contained in a single plane. The tri-

lateration reconstruction method is illustrated in the right panel of Fig. 3. Knowing the emission and annihilation position of the positron, one can reconstruct the direction of motion of the positron and, hence, the direction of the spin for the positronium.

In the case of the ^{22}Na source, the average degree of the positronium polarization is equal to $P = \langle v \rangle / c = 0.67$, and for ^{68}Ge polarization P amounts to 0.9 [6, 80]. This polarization is to large extent preserved during the thermalization process [81]. Its losses in the material are estimated to be about 17% for positrons from ^{68}Ge and 8% for positrons from ^{22}Na [82]. Taking into account that only 2/3 of created ortho-positronium atoms possess spins parallel to the spins of the positrons [15], it was estimated that the average polarization of ortho-positronium (achievable by irradiating the porous materials with positrons from the beta-plus isotope) is equal to about 0.41 when using ^{22}Na and 0.50 when applying ^{68}Ge [6, 82]. For positrons emitted in the cone with an opening angle of 2α, the average polarization is decreased by a factor of $(1 + \cos(\alpha))/2$ [80]. Therefore, in practice, the polarization degree is further lowered due to the finite angular resolution of the determination of the positrons direction.

With the cylindrical target and the J-PET detector shown schematically in the right panel of Fig. 2 and the right panel of Fig. 3, respectively, we can achieve an angular resolution for the positron direction determination of about 15° [61]. Therefore, the loss of polarization due to the uncertainty of the determination of positron direction will amount to about 2% only. In the case of the Gammasphere experiment, the annihilation points were not reconstructed, so only a polarization averaged over the total hemisphere was used, thus leading to an effective polarization loss by a factor of two.

4.3. Tensor spin-polarized source of positronium atoms

Tensor polarization of o-Ps atoms is defined as

$$P_2 = (N_{+1} - 2N_0 + N_{-1})/(N_{+1} + N_0 + N_{-1}), \tag{1}$$

where N_{+1}, N_0, and N_{-1} denote the number of atoms with spin projection along the quantization axis equal to $+1$, 0 and -1, respectively. The quantization axis will be provided by the direction of the external magnetic field. Each of the spin projection can occur with the same probability. A non-zero value of tensor polarization may be effectively generated by the off-line selection of events corresponding to decays of ortho-positronium in the static magnetic field. The method makes use of the fact that in the magnetic field the o-Ps state with $m = 0$ mixes with p-Ps. This mixing changes significantly the lifetime of o-Ps in $m = 0$ state. *E.g.* in the magnetic field of 5 kG, in a aerogel the o-Ps ($m = 0$) lifetime decreases from about 126 ns to

about 22 ns [5], whereas the lifetime of o-Ps states with $m = +1$ or $m = -1$ is not affected by the magnetic field. Therefore, by choosing a lifetime interval of o-Ps one can vary the ratio of N_0 to $(N_{+1} + N_{-1})$ and, hence, vary the polarization P_2. By using a magnetic field of ~ 5 kG and a time window from 50 to 130 ns (in aerogel), a polarization degree of $P_2 = 0.87$ was achieved in the experiment described in reference [5]. The design of a proper system for the generation of the static magnetic field is one of the tasks being presently realized by the J-PET Collaboration. The first preliminary studies by means of the Vizimag simulation software indicate that using a method of active shielding allows to generate a field in the order of 1 T at the source in the center of the detector with the fringe field less than the Earth's magnetic field at the photomultipliers (distant by about 60 cm). Problems with photomultipliers in the magnetic field can be reduced by using a SiPM readout [83].

4.4. Monitoring of ortho-positronium spin polarization

In the case of the tensor polarization, the quantization axis is defined by the direction of the magnetic field, and in the case of the linear polarization, we can determine it on the event-by-event basis as a direction of the positron motion. The degree of the tensor polarization may be monitored based on the measurement of the angular distribution between the normal to the decay plane and the quantization axis, where the decay plane is defined as the plane containing momenta of photons from the o-Ps $\to 3\gamma$ decay. The distribution of the angle θ_S between the spin direction of o-Ps and the normal to the decay plane is proportional to the term $(1 + \cos^2 \theta_S)$ for $m = 0$, and to the term $\frac{1}{2}(3 - \cos^2 \theta_S)$ for $m = \pm 1$ [84]. Therefore, we can determine the degree of the tensor polarization by the comparison of the angular distribution of the normal to the decay plane with respect to the direction of the magnetic field for the cases when magnetic field is switched on and off. Without magnetic field, an isotropic distribution is expected and with the magnetic field, the polarization degree will be derived from the amplitude of the term proportional to $\cos^2 \theta_S$. In the extreme cases if $P_2 = -2$, the expected distribution should be proportional to $(1 + \cos^2 \theta_S)$, whereas for $P_2 = 1$ it should behave as $(3 - \cos^2 \theta_S)$. We can also control how the degree of the tensor polarization changes with the lifetime interval of o-Ps chosen in the analysis.

The angular distribution of θ_S can be also used to control the systematic uncertainties in the case of the studies with the linearly spin-polarized o-Ps. For example, by the comparison of the angular distributions when using different positron sources (e.g. such as ^{22}Na and ^{68}Ge) as it was done in the case of the Gammasphere experiment [6].

4.5. Polarization of photons

J-PET scanner is built of plastic scintillators strips. Therefore, photons from the positronium decay are interacting via Compton effect and a fraction of them may undergo two or more scatterings in different strips (see Fig. 3 and reference [85]). Since gamma quantum is a transverse electromagnetic wave, and since Compton scattering is at most likely in the plane perpendicular to the electric vector of the photon [86, 87], we can determine the direction of its linear polarization $\vec{\epsilon}_i$ *e.g.* by constructing $\vec{\epsilon}_i = \vec{k}_i \times \vec{k}_i'$, where $\vec{k}_i$ and $\vec{k}_i'$ denote momentum vectors of ith gamma quantum before and after the Compton scattering, respectively (as indicated in Fig. 3). The ortho-positronium decay plane and the scattering plane for one of the photons are shown schematically in Fig. 4. θ denotes the scattering angle between the directions of propagation of the primary photon $\vec{k}$ and the scattered photon $\vec{k}'$. It is important to note that, independently of the value of θ, the probability of the scattering has its maximum value when the scattering plane is perpendicular to the direction of the electric vector of the primary photon ($\eta = 90°$). The corresponding cross section reads [86, 87]

$$d\sigma/d\Omega \sim (k'/k)^2 \left(k/k' + k'/k - 2\sin^2\theta \, \cos^2\eta \right) , \qquad (2)$$

where the meaning of the angles is explained in Fig. 4. The above formulae indicates that this probability is maximum for ($\eta = 90°$), but it is not necessarily vanishing when the scattering plane is parallel to $\vec{\epsilon}$. Lower left panel of Fig. 4 indicates the ratio of $[d\sigma/d\Omega(\eta = 90°)]/[d\sigma/d\Omega(\eta = 0°)]$ as a function of the scattering angle θ. Energy of photons from the o-Ps $\to 3\gamma$ decays ranges from 0 to 511 keV. In this energy range, the ratio changes significantly. For example, for the 511 keV photons, it is maximal at θ of about 82° and for photons with energy of 100 keV the maximum is at about 89°. The dependences of $d\sigma/d\Omega$ on the η angle are shown in the right panel of Fig. 4. This dependence of the cross sections sets the limit for the achievable resolution for the determination of the direction of the $\vec{\epsilon}$ with the Ansatz that $\vec{\epsilon}_i = \vec{k}_i \times \vec{k}_i'$. At present, a quantitative estimation is ongoing. However, it is worth to stress that, independently of the determination of the photons polarization, the ability of the J-PET detector to determine the angle ϕ between the decay and scattering planes, as well as the angles between o-Ps spin and the scattering planes of photons opens possibilities for experimental definition of orthogonal states of photon and, hence, enables studies of the multi-partite entanglement of high energy photons originating from the positronium annihilation [88].
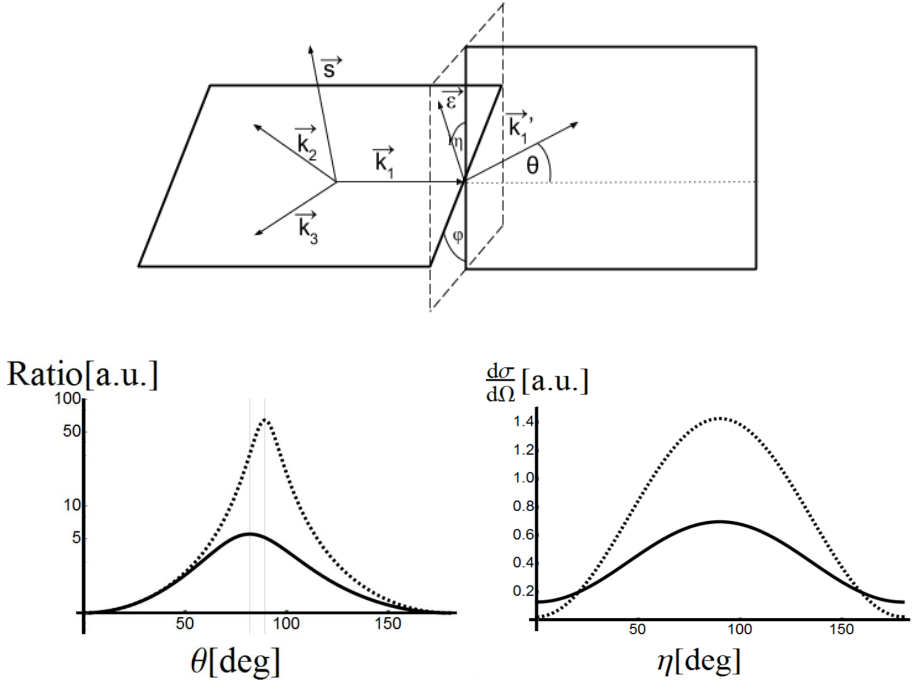
Fig. 4. (Upper panel) Schematic illustration of the decay plane of ortho-positronium and the scattering plane of one of the photons. $\vec{k_i}$ denotes momentum vector of ith photon, $\vec{\epsilon}$ denotes the electric vector of photon, θ stands for the scattering angle, ϕ indicates angle between the decay plane of ortho-positronium and the scattering plane of the photon denoted by $\vec{k_1}$. η denotes the angle between the scattering plane and the electric vector of photon with momentum $\vec{k_1}$, and $\vec{S}$ indicates the spin of ortho-positronium. (Lower left) A ratio of $[d\sigma/d\Omega(\eta = 90°)]/[d\sigma/d\Omega(\eta = 0°)]$ as a function of the scattering angle θ. Solid line represents result for $k_1 = 511$ keV, and dashed line for $k_1 = 100$ keV. (Lower right) $d\sigma/d\Omega$ in arbitrary units shown as a function of the η angle for the θ fixed to 82° in the case of the 511 keV photon (solid line) and for θ fixed to 89° in the case of the 100 keV photon (dashed line).

4.6. Application of the PALS method with the J-PET detector

The J-PET detector enables to determine the lifetime of produced positronium atoms on the event-by-event basis. For this purpose, not only photons from the e^+e^- annihilation but also the de-excitation photon from the excited daughter nucleus originating from the beta-plus decay will be registered. This will permit to measure differences between the time of formation and the time of annihilation of positronium atoms. These times can be reconstructed since with the J-PET detector, we can reconstruct hit-time and

hit-position of the photons, as well as the annihilation position [61, 79, 89]. In the case of unpolarized source, for the time of formation of the positronium atom, we will use the reconstructed time of the emission of the de-excitation photon. This approximation leads to negligible uncertainties, since the time between the emission of the positron and the formation of the positronium, as well as the average lifetime of the ^{22}Ne* excited nucleus (^{22}Na $\rightarrow^{22}$ Ne* $e^+ \nu_e \rightarrow^{22}$ Ne $\gamma\, e^+ \nu_e$), are in the order of few ps. Due to the momentum conservation, the three photons from the o-Ps decay will move inside a plane comprising the annihilation point (Fig. 5 (left)). However, the direction of movement of the de-excitation quantum, not being correlated with the annihilation photons, will be distributed isotropically with respect to the decay plane. The annihilation and de-excitation photons can be disentangled based on the combination of at least three criteria: *(i)* the measured energy deposition, *(ii)* the distance between the decay plane and the annihilation place, and *(iii)* the hit-time difference which is fixed for a given annihilation and hit-positions for annihilation photons. Figure 5 (right) shows energy loss spectrum expected for the highest energy photons from the positronium annihilation compared to the spectra expected from the de-excitation photons from ^{22}Na isotope. The results were obtained taking into account the experimental energy resolution of the J-PET detector [62].
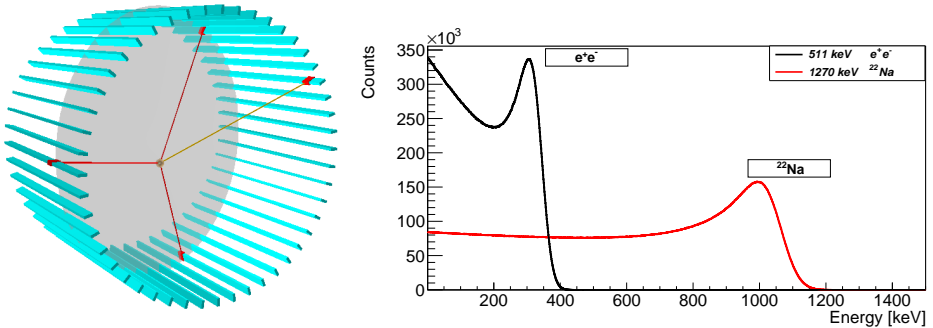

Fig. 5. (Left) Schematic view of the inner layer of the J-PET detector with superimposed decay plane of o-Ps $\rightarrow 3\gamma$ process. Lines inside the plane indicate annihilation photons and the line pointing out of the plane indicates a de-excitation photon used for the start time determination. (Right) Simulated energy loss spectra for annihilation (0.511 MeV) and de-excitation photons from the ^{22}Na decay (1.27 MeV). The shown distributions include the energy resolution of the J-PET detector [62].

4.7. Simulations of o-Ps → 3γ decays

Simulation-based studies are the subject of the ongoing research of the J-PET Collaboration. However, here we present preliminary results which show that the competing accuracy with respect to the previous experiments can be achieved for the discussed studies. Simulations are conducted using the Geant4 Application for Tomographic Emission (GATE) [85] supplemented with our own simulation procedures which are necessary in order to account for annihilation processes to more than 2γ, because such processes are not included in the standard commonly applied simulation packages. The J-PET detector is based on the plastic scintillators and, in practice, due to the low atomic number of this material, photons in the energy range between 50 keV and 511 keV interact predominantly via the Compton effect. We have simulated the response of the detector to o-Ps → 3γ process taking into account: *(i)* the energy dependence of the o-Ps → 3γ transition amplitude according to the predictions based on the quantum electrodynamics [90], *(ii)* the energy dependence of the total cross section for the Compton scattering, *(iii)* the energy distribution of the scattered electrons, *(iv)* the geometry of the J-PET system as well as its energy resolution [62]. The correctness of the simulation procedures was corroborated by the comparison between measured and simulated distributions for 511 keV photons [58]. The details of the simulations will be described in the forthcoming article [91].

4.8. Reduction of the instrumental background

The J-PET detector was designed for the medical imaging purposes and it allows for the identification of the $e^+e^- \to 2\gamma$ events. In addition, the very good angular resolution of about one degree and time resolution of about 100 ps of the J-PET detector allows for the significant suppression of the background also for the studies of o-Ps → 3γ events. Here, we show only rough estimations in order to demonstrate the background suppression capability of the J-PET system. The most dangerous instrumental background is due to the secondary scattering of photons originating from the 2γ events which may mimic the registration of 3γ. However, we can disentangle true and false 3γ events based on: *(i)* the relation between position of the individual detectors (ID) and the time difference between registered hits (Δt), *(ii)* the angular correlation of angles between the direction of photons, and *(iii)* the distance between the origin of the annihilation (position of the annihilation chamber) and the decay plane. In Fig. 6, we show two example spectra with the expected ΔID *versus* Δt and θ_{23} *versus* θ_{12} distributions for o-Ps → 3γ events with the superimposed distributions originating from the $e^+e^- \to 2\gamma$ events which resulted in three hits in the detector. For the true o-Ps → 3γ events, the Δt between different hits in the detector should

be equal to zero and, therefore, the true and false 3γ events only slightly overlap. Similarly, after ordering the relative angles ($\theta_{12} < \theta_{23} < \theta_{31}$), the true and false events have very small (almost none) overlap region at the θ_{23} *versus* θ_{12} correlation plot. Applying relatively conservative criteria on all of these mentioned observables (*e.g.* $\theta_{23} > 185 - \theta_{12}$ and $\Delta t < 0.3$ ns at Fig. 6), we expect to reduce the background from 2γ annihilation by a factor larger than 10^9 (including detection acceptance and efficiency). This high reduction of background is crucial because the efficiency for the simultaneous detection of 3γ from the o-Ps decay is small.
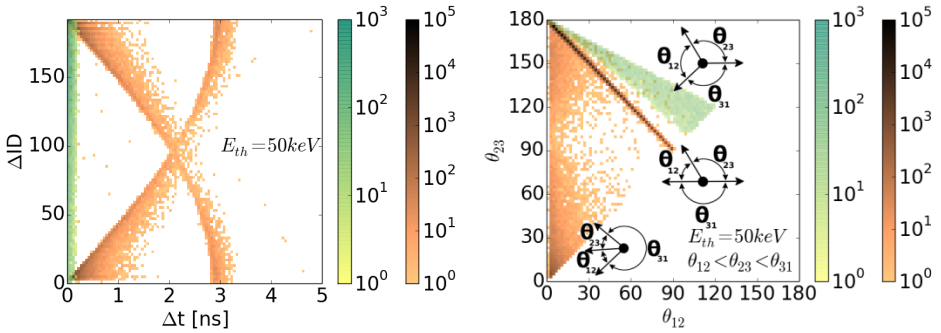

Fig. 6. (Left) Simulated distributions of differences between detectors ID (ΔID) and differences of hit-times (Δt) for events with three hits registered from the annihilation $e^+e^- \to 2\gamma$ (points concentrated in diagonal and anti-diagonal bands) and o-Ps $\to 3\gamma$ (points concentrated in vertical band close to $\Delta t = 0$). The module ID increases monotonically with the growth of the azimuthal angle between the vertical direction and the line connecting the center of the J-PET detector and a given module [85]. (Right) Distribution of relative angles between reconstructed directions of photons. The numbering of photons was assigned such that $\theta_{12} < \theta_{23} < \theta_{31}$. Shown distributions were obtained requiring three hits each with energy deposition larger than $E_{th} = 50$ keV. Points below and at diagonal band show results for simulations of $e^+e^- \to 2\gamma$ and points above the diagonal band correspond to o-Ps $\to 3\gamma$. Typical topology of o-Ps $\to 3\gamma$ and two kinds of background events are indicated. The figures are adapted from [85, 92].

4.9. Physical background due to the positronium production method

Due to the short lifetime of p-Ps (0.125 ns) and short average time of direct annihilations (about 0.5 ns), their misidentification as o-Ps $\to 3\gamma$ events can be reduced to a negligible level by the requirement that the time difference between the de-excitation and annihilation photons is larger than *e.g.* 50 ns as used *e.g.* in reference [5]. However, such condition does not eliminate the background contributions originating from interactions of o-Ps with electrons at the surfaces of voids in the porous material. The rate

of this kind of o-Ps loss may be estimated from its lifetime in the material used for the target, and *e.g.* in the XAD-4 porous polymer [74], it is equal to $(1 - \tau_{\text{aero}}/\tau_{\text{vacuum}}) = (1 - 91/142) \approx 0.36$, and for the aerogel IC3100, it amounts to about 0.07. Thus, about 7% to 36% of o-Ps may undergo pick-off annihilations or ortho–para spin conversion (due to the spin–orbit interaction or due to electron exchange). Further on, we will assume that each of these processes contributes by 20%, however, it is important to stress that this is a very conservative assumption since *e.g.* conversion processes are strongly suppressed in the aerogels in vacuum as it will be in our case.

In principle, the sample of events recognized as originating from o-Ps decay ($N_{\text{o}-\text{Ps}}$) would include events from the following processes: true decays of o-Ps $\rightarrow 3\gamma$ ($N_{\text{o}-\text{Ps}} \rightarrow 3\gamma$); pick-off with subsequent prompt annihilation to 3γ ($N_{3\gamma-\text{pick-off}}$); pick-off with subsequent prompt annihilation to 2γ misidentified as 3γ due to secondary scatterings ($N_{2\gamma-\text{pick-off}}$); conversion of o-Ps to p-Ps with subsequent C-symmetry violating decay to 3γ ($N_{3\gamma-\text{conv}}$); and conversion of o-Ps to p-Ps with subsequent annihilation to 2γ misidentified as 3γ due to the secondary scatterings ($N_{2\gamma-\text{conv}}$). Taking into account the upper limits for the C-symmetry violations, the detection and reconstruction efficiencies, as well as the background suppression discussed above, we found that the largest contribution (by almost two orders of magnitude larger than the others) which may mimic the symmetry violation originates from the pick-off process with subsequent prompt annihilation to 3γ ($N_{3\gamma-\text{pick-off}}$). The conservative upper limit of this background contribution may be estimated as: $N_{3\gamma-\text{pick-off}}/N_{\text{o}-\text{Ps}} < 0.2/370 \approx 5 \times 10^{-4}$.

The experiment described in this article aims at the determination of the expectation value of correlation operators which are odd with respect to the studied symmetries. The non-zero values of such operators would reflect at the non-zero asymmetry of counts defined appropriately for each studied symmetry. It is a matter of further investigations to estimate a possible asymmetry due to the background discussed above. However, assuming arbitrarily but rather conservatively that the asymmetry of 3γ–pick-off background is less than 10%, we would obtain the systematic uncertainty of about 5×10^{-5} which is by two orders of magnitude lower than the present experimental limits [5, 6]. Moreover, it should be stressed that the measurement of the true 2γ events with high statistics will allow for the precise control of the amount of this background contribution. In addition, the possible contribution to this asymmetry from the true o-Ps $\rightarrow 3\gamma$ decays and the background events can be disentangled by the comparison of results obtained for materials with different voids sizes. The asymmetry originating from the background contributions changes with the void size, whereas the contribution from the true o-Ps $\rightarrow 3\gamma$ decay remains constant. Therefore, we expect to reach a systematic sensitivity below 5×10^{-5}.

5. Observables for the discrete symmetries

We intend to test discrete symmetries by the determination of the expectation value of the operators listed in Table I. Observation of the non-zero expectation value of any of these operators would imply a non-invariance of these symmetries for which the given operator is odd-symmetric (marked in the table with "$-$"). For example, the CPT symmetry may be tested by measuring the angular correlations between the spin of the ortho-positronium atom and its decay plane. CPT-symmetry breaking may manifest itself as an asymmetry of the $\vec{S} \cdot (\vec{k_1} \times \vec{k_2})$ operator. Its non-zero expectation value

TABLE I

Operators for the o-Ps $\rightarrow 3\gamma$ process and their properties with respect to the C, P, T, CP and CPT symmetries. New operators (including $\vec{\epsilon}$) available at J-PET are shown in the last three rows.

Operator	C	P	T	CP	CPT
$\vec{S} \cdot \vec{k_1}$	$+$	$-$	$+$	$-$	$-$
$\vec{S} \cdot \left(\vec{k_1} \times \vec{k_2} \right)$	$+$	$+$	$-$	$+$	$-$
$\left(\vec{S} \cdot \vec{k_1} \right) \left(\vec{S} \cdot \left(\vec{k_1} \times \vec{k_2} \right) \right)$	$+$	$-$	$-$	$-$	$+$
$\vec{k_2} \times \vec{\epsilon_1}$	$+$	$+$	$-$	$-$	$+$
$\vec{S} \cdot \vec{\epsilon_1}$	$+$	$+$	$-$	$+$	$-$
$\vec{S} \cdot \left(\vec{k_2} \times \vec{\epsilon_1} \right)$	$+$	$-$	$+$	$-$	$-$

signals a difference in the probability between cases when spin vector $\vec{S}$ of o-Ps atom is pointing up and down with respect to the normal to the decay plane defined as $\vec{k_1} \times \vec{k_2}$. Thus, CPT-symmetry violation would manifest itself as an asymmetry in the decay plane orientation with respect to the initial spin of the o-Ps atom. The decay plane may be oriented by the ordering of photons according to the descending momentum: $k_1 > k_2 > k_3$. J-PET detector does not allow for the direct measurement of the photon energy. However, we can reconstruct the momentum of each photon from the o-Ps $\rightarrow 3\gamma$ process based on the measurement of the hit-positions and annihilation point which allows for the determination of the relative angles between the photons. The reconstruction of these angles and the use of energy and momentum conservations permit to reconstruct the momenta of all decay photons. As preparatory studies, we have performed Monte Carlo simulations of the response of the J-PET detector to the o-Ps $\rightarrow 3\gamma$ decay and reconstructed the photons energies and propagation angles. Taking into account the experimentally determined position and time resolutions of the detector [58, 62], we have obtained angular resolution of about 1 degree and energy resolution of about 5 keV [91].

In order to test the C symmetry, we will search for the C-violating decays of ortho-positronium (o-Ps $\to 4\gamma$) and para-positronium (p-Ps $\to 3\gamma$). However, to reach a higher sensitivity in the studies of the C-symmetry violation not only will the number of photons be taken into account, but we will also make the comparison between symmetric and asymmetric configurations of photons. We will take advantage of the fact that para-positronium decay p-Ps $\to 3\gamma$ in the symmetric configuration (with photons emitted with directions towards the vertices of the equilateral triangle) is forbidden not only by the C symmetry but also by the Bose–Einstein statistics and rotational symmetry (angular momentum conservation) [9]. Therefore, the C-symmetry violation in the p-Ps $\to 3\gamma$ decay may also manifest itself as a variation of the ratio of 3γ decays in the symmetric and non-symmetric configurations, while the ratio of ortho-positronium to para-positronium is varied. The latter may be achieved by the variation of the gas pressure in the positronium production targets or by the variation of the static magnetic field inside the target. The time resolution of the J-PET tomograph of about 0.1 ns [62] will be of great advantage in selecting smaller time window corresponding to the production of para-positronium and hence in reducing the background from the C-allowed decays of ortho-positronium o-Ps $\to 3\gamma$. Analogously, it is favorable to study the C-symmetry violation via the comparison of the o-Ps $\to 4\gamma$ decay rate into symmetric and non-symmetric configurations. In this case, in the symmetric configuration, photons are emitted along the directions defined by the vertices of the tetrahedron. The C-allowed decay p-Ps $\to 4\gamma$ into symmetric configuration is forbidden via rotational symmetry [93]. Therefore, the physical background due to the C-allowed o-Ps $\to 4\gamma$ decay is negligible in this symmetric configuration and thus only an instrumental background will limit the accuracy. In addition, in the tetrahedral configuration, a C-symmetry violation in o-Ps $\to 4\gamma$ decay is expected to be maximal [93, 94].

6. Summary

The Jagiellonian Positron Emission Tomograph (J-PET) was constructed as a prototype of a cost-effective scanner for the simultaneous metabolic imaging of the whole human body [58, 62, 83]. It is optimized for the detection of photons from the electron–positron annihilation with high time- and angular-resolutions, thus providing new opportunities for research with photons originating from the decays of positronium atoms in fundamental physics, as well as in life and material sciences [95–98].

The C, CP, T and CPT symmetries are of fundamental importance in physics. Violation of T or CP invariance in purely leptonic systems have never been seen so far. Based on known mechanisms of C and CP violations, one cannot explain the large asymmetry between matter and anti-

matter in the observable Universe. The above facts constitute motivation for the elaboration of the experimental proposal presented in this article which comprises studies of asymmetries between leptons and anti-leptons at low energies with the J-PET detector. In this article, we described the potential of the J-PET detector for tests of C, CP, T and CPT symmetries in the decays of para- and ortho-positronium atoms. The tests will be based on the determination of the expectation values of the discrete-symmetries-odd operators which may be constructed from the momentum and polarization vectors of photons and from the spin vector of ortho-positronium atom.

With respect to the previous experiments performed with crystal based detectors, J-PET built of plastic scintillators, provides superior time resolution, higher granularity, lower pile-ups, and opportunity of determining photon's polarization. These features allow us to expect improvement by more than an order of magnitude in tests of discrete symmetries in decays of positronium atoms.

REFERENCES

[1] A.D. Sakharov, *Pis'ma Zh. Eksp. Teor. Fiz.* **5**, 32 (1967).

[2] D.N. Spergel *et al.*, *Astrophys. J. Suppl.* **148**, 175 (2003) [arXiv:astro-ph/0302209].

[3] M. Fukugita, T. Yanagida, *Phys. Lett. B* **174**, 45 (1986).

[4] W. Buchmuller, T. Yanagita, *Annu. Rev. Nucl. Part. Sci.* **55**, 311 (2005) [arXiv:hep-ph/0502169].

[5] T. Yamazaki *et al.*, *Phys. Rev. Lett.* **104**, 083401 (2010) [arXiv:0912.0843 [hep-ex]].

[6] P.A. Vetter, S.J. Freedman, *Phys. Rev. Lett.* **91**, 263401 (2003).

[7] W. Bernreuther *et al.*, *Z. Phys. C* **41**, 143 (1988).

[8] M. Deutsch, *Phys. Rev.* **82**, 455 (1951), Nobel Prize in 1956.

[9] M.S. Sozzi, *Discrete Symmetries and CP Violation. From Experiment to Theory*, Oxford University Press, 2008.

[10] A.H. Al-Ramadhan, D.W. Gidley, *Phys. Rev. Lett.* **72**, 1632 (1994).

[11] R.S. Vallery, P.W. Zitzewitz, D.W. Gidley, *Phys. Rev. Lett.* **90**, 203402 (2003).

[12] O. Jinnouchi, S. Asai, T. Kobayashi, *Phys. Lett. B* **572**, 117 (3003).

[13] K.A. Olive *et al.* [Particle Data Group], *Chin. Phys. C* **38**, 090001 (2014).

[14] J. McDonough *et al.*, *Phys. Rev. D* **38**, 2121 (1988).

[15] B.K. Arbic *et al.*, *Phys. Rev. A* **37**, 3189 (1988).

[16] J. Yang *et al.*, *Phys. Rev. A* **54**, 1952 (1996).

[17] A.P. Mills, S. Berko, *Phys. Rev. Lett.* **18**, 420 (1967).

[18] P.A. Vetter, S.J. Freedman, *Phys. Rev. A* **66**, 052505 (2002).

[19] J.H. Christenson, J.W. Cronin, V.L. Fitch, R. Turlay, *Phys. Rev. Lett.* **13**, 138 (1964).

[20] D. Babusci *et al.*, *Phys. Lett. B* **723**, 54 (2013) [arXiv:1301.7623 [hep-ex]].

[21] M. Silarski, Ph.D. Thesis, Jagiellonian University, 2012 [arXiv:1302.4427 [hep-ex]].

[22] A. Abashian *et al.*, *Phys. Rev. Lett.* **86**, 2509 (2001) [arXiv:hep-ex/0102018].

[23] B. Aubert *et al.*, *Phys. Rev. Lett.* **86**, 2515 (2001) [arXiv:hep-ex/0102030].

[24] M. Kobayashi, T. Maskawa, *Prog. Theor. Phys.* **49**, 652 (1973), Nobel Prize in 2008.

[25] N. Cabibbo, *Phys. Rev. Lett.* **10**, 531 (1963).

[26] R. Aaij *et al.*, *Eur. Phys. J. C* **73**, 2373 (2013) [arXiv:1208.3355 [hep-ex]].

[27] I. Adachi *et al.*, *JINST* **9**, C07017 (2014).

[28] T. Durt, A. Di Domenico, B. Hiesmayr, arXiv:1512.08437 [quant-ph].

[29] B.C. Hiesmayr *et al.*, *Eur. Phys. J. C* **72**, 1856 (2012).

[30] B.C. Hiesmayr, *Found. Phys. Lett.* **14**, 231 (2001).

[31] B.C. Hiesmayr, *J. Phys.: Conf. Ser.* **631**, 012067 (2015).

[32] P. Adlarson *et al.*, arXiv:1509.06588 [nucl-ex].

[33] G. Amelino-Camelia *et al.*, *Eur. Phys. J. C* **68**, 619 (2010) [arXiv:1003.3868 [hep-ex]].

[34] D.S. Ayres *et al.*, arXiv:hep-ex/0503053; J. Bian, arXiv:1309.7898 [physics.ins-det].

[35] K. Abe *et al.*, *Phys. Rev. Lett.* **112**, 061802 (2014) [arXiv:1311.4750 [hep-ex]].

[36] M. Ghosh *et al.*, *Nucl. Phys. B* **884**, 274 (2014) [arXiv:1401.7243 [hep-ph]].

[37] M. Ghosh *et al.*, *Phys. Rev. D* **89**, 011301(R) (2014)
[arXiv:1306.2500 [hep-ph]].

[38] C.A. Baker *et al.*, *Phys. Rev. Lett.* **97**, 131801 (2006)
[arXiv:hep-ex/0602020].

[39] H.Y. Cheng, *Phys. Rev. D* **28**, 150 (1983).

[40] S.N. Gninenko, N.V. Krasnikov, A. Rubbia, *Mod. Phys. Lett. A* **17**, 1713
(2002).

[41] J. Bernabeu, F. Martinez-Vidal, *Rev. Mod. Phys.* **87**, 165 (2015)
[arXiv:1410.1742 [hep-ph]].

[42] J.P. Lees *et al.*, *Phys. Rev. Lett.* **109**, 211801 (2012)
[arXiv:1207.5832 [hep-ex]].

[43] J. Bernabeu F. Martínez-Vidal, P. Villanueva-Pérez, *J. High Energy Phys.*
1208, 64 (2012) [arXiv:1203.0171 [hep-ph]].

[44] J.S. Bell, *Proc. R. Soc. London Ser. A* **231**, 479 (1955).

[45] G. Lüders, *Ann. Phys.* **2**, 1 (1957); *Ann. Phys. (N.Y.)* **281**, 1004 (2000).

[46] O.W. Greenberg, *Phys. Rev. Lett.* **89**, 231602 (2002)
[arXiv:hep-ph/0201258].

[47] S. Hawking, *Commun. Math. Phys.* **87**, 395 (1982).

[48] V.A. Kostelecky, N. Russell, *Rev. Mod. Phys.* **83**, 11 (2011)
[arXiv:0801.0287 [hep-ph]].

[49] A. Di Domenico, *Frascati Phys. Ser.*, Vol. XLIII (2007).

[50] D.F. Phillips *et al.*, *Phys. Rev. D* **63**, 111101 (2001)
[arXiv:physics.atom-ph/0008230].

[51] G. Gabrielse *et al.*, *Phys. Rev. Lett.* **82**, 3198 (1999).

[52] G. Gabrielse *et al.*, *Phys. Rev. Lett.* **108**, 113002 (2012).

[53] J. DiSciacca *et al.*, *Phys. Rev. Lett.* **110**, 130801 (2013).

[54] D. Babusci *et al.*, *Phys. Lett. B* **730**, 89 (2014)
[arXiv:1312.6818 [hep-ex]].

[55] J. Bernabeu, A. Di Domenico, P. Villanueva-Perez, *Nucl. Phys. B* **868**, 102
(2013) [arXiv:1208.0773 [hep-ph]].

[56] P. Moskal, Patent number: WO2011008118-A2, PL388556-A1,
US2012175523-A1, EP2454611-A2, JP2012533733-W.

[57] P. Moskal, Patent number: WO2011008119-A2; PL388555-A1;
US2012112079-A1; EP2454612-A2; JP2012533734-W.

[58] P. Moskal *et al.*, *Nucl. Instrum. Methods Phys. Res. A* **775**, 54 (2015)
[arXiv:1412.6963 [physics.ins-det]].

[59] L. Raczyński *et al.*, *Nucl. Instrum. Methods Phys. Res. A* **764**, 186 (2014)
[arXiv:1407.8293 [physics.ins-det]].

[60] L. Raczyński *et al.*, *Nucl. Instrum. Methods Phys. Res. A* **786**, 105 (2015)
[arXiv:1503.05188 [physics.ins-det]].

[61] A. Gajos *et al.*, Patent number: PCT/PL2015/050038; submitted to *Nucl. Instrum. Methods Phys. Res. A*.

[62] P. Moskal *et al.*, *Nucl. Instrum. Methods Phys. Res. A* **764**, 317 (2014) [arXiv:1407.7395 [physics.ins-det]].

[63] M. Pałka, P. Moskal, Patent number: WO2015028600-A1.

[64] M. Pałka *et al.*, *Bio-Algorithms and Med-Systems* **10**, 41 (2014) [arXiv:1311.6127 [physics.ins-det]].

[65] G. Korcyl, P. Moskal, M. Kajetanowicz, M. Pałka, Patent number: WO2015028594-A1.

[66] G. Korcyl *et al.*, *Acta Phys. Pol. B* **47**, 491 (2016), this issue.

[67] G. Korcyl *et al.*, *Bio-Algorithms and Med-Systems* **10**, 37 (2014).

[68] W. Krzemień *et al.*, *Nukleonika* **60**, 745 (2015) [arXiv:1508.02751 [physics.ins-det]].

[69] W. Krzemień *et al.*, *Acta Phys. Pol. A* **127**, 1491 (2015) [arXiv:1503.00465 [physics.ins-det]].

[70] W. Krzemień *et al.*, *Acta Phys. Pol. B* **47**, 561 (2016), this issue.

[71] N. Sharma *et al.*, *Nukleonika* **60**, 765 (2015) [arXiv:1508.07463 [physics.ins-det]].

[72] P. Moskal *et al.*, *Acta Phys. Pol. A* **127**, 1495 (2015) [arXiv:1502.07886 [physics.ins-det]].

[73] K. Szkliniarz *et al.*, *Acta Phys. Pol. A* **127**, 1471 (2015).

[74] B. Jasińska *et al.*, *Acta Phys. Pol. B* **47**, 453 (2016), this issue.

[75] R. Ferragut *et al.*, *J. Phys.: Conf. Ser.* **225**, 012007 (2010).

[76] G. Consolati *et al.*, *Chem. Soc. Rev.* **42**, 3821 (2013).

[77] C.J. Edwardson *et al.*, *J. Phys.: Conf. Ser.* **262**, 012018 (2011).

[78] A. Kierys *et al.*, *Microporous Mesoporous Mater.* **179**, 104 (2013).

[79] A. Gajos, Diploma Thesis, Jagiellonian University, 2013.

[80] P. Coleman, *Positron Beams and Their Applications*, World Scientific, 2000.

[81] J. Van House, P.W. Zitzewitz, *Phys. Rev. A* **29**, 96 (1984); P.W. Zitzewitz *et al.*, *Phys. Rev. Lett.* **43**, 1281 (1979).

[82] J. Yang *et al.*, *Jpn. J. Appl. Phys.* **36**, 3764 (1997).

[83] P. Moskal *et al.*, *Phys. Med. Biol.* **61**, 2025 (2016) [arXiv:1602.02058 [physics.ins-det]].

[84] W. Bernreuther, O. Nachtmann, *Z. Phys. C* **11**, 235 (1981).

[85] P. Kowalski *et al.*, *Acta Phys. Pol. A* **127**, 1505 (2015) [arXiv:1502.04532 [physics.ins-det]].

[86] O. Klein, T. Nishina, *Z. Phys.* **52**, 853 (1929).

[87] R.D. Evans, *Corpuscles and Radiation in Matter II*, Springer, Berlin–Heidelberg 1958, pp. 218–298.

[88] B. Hiesmayr *et al.*, in preparation.

[89] A. Gajos, *Frascati Phys. Ser.* **59**, 25 (2014) [arXiv:1409.2132 [hep-ex]]; *Acta Phys. Pol. B* **46**, 13 (2015) [arXiv:1501.04801 [hep-ex]].

[90] V.B. Berestetskii, E.M. Lifshitz, L.P. Pitaevskii, *Relativistic Quantum Theory*, Pergamon Press, 1971.

[91] D. Kamińska *et al.*, in preparation.

[92] D. Kamińska *et al.*, *Nukleonika* **60**, 729 (2015) [arXiv:1509.01114 [physics.ins-det]].

[93] A. Rich, *Rev. Mod. Phys.* **53**, 127 (1981).

[94] H.S. Mani, A. Rich, *Phys. Rev. D* **4**, 122 (1971).

[95] P. Moskal, Patent number: WO2015028604, PCT/EP2014/068374.

[96] E. Kubicz *et al.*, *Nukleonika* **60**, 749 (2015) [arXiv:1509.00411 [q-bio.OT]].

[97] A. Wieczorek *et al.*, *Acta Phys. Pol. A* **127**, 1487 (2015) [arXiv:1502.02901 [physics.ins-det]].

[98] A. Wieczorek *et al.*, *Nukleonika* **60**, 777 (2015) [arXiv:1508.06820 [physics.ins-det]].